An in-phantom dosimetry system using pin silicon photodiode radiation sensors for measuring organ doses in x-ray CT and other diagnostic radiology

Takahiko Aoyama,[a] Shuji Koyama, and Chiyo Kawaura
School of Health Sciences, Nagoya University, Daikominami, Higashi-ku, Nagoya 461-8673, Japan

(Received 3 October 2001; accepted for publication 3 May 2002; published 20 June 2002)

A dosimetry system using commercially available pin silicon photodiodes as the sensor is evaluated for in-phantom dose measurements in x-ray CT and other diagnostic radiology. System sensitivity measured as a function of the effective energy of x rays was between 0.37 and 0.49 V/mGy at an effective energy range between 23.5 and 72 keV. The minimum detectable organ dose with 25% uncertainty was estimated to be 0.02 mGy. The excellent output linearity was found over a dose range from 0.03 to more than 10 mGy with flat dose rate response of system sensitivity up to 35 $mGy\,s^{-1}$, though the sensitivity indicated some energy dependence across the diagnostic energy range with a maximum of about 10%/10 keV. Since angular dependence of the sensitivity of the photodiode sensor was found to be small enough it would induce negligible dose error. Dose profile measurement along the axis of a thoracic phantom undergoing CT chest examination indicated the reliability of dose values over a range of two orders of magnitude from less than 0.2 to 12 mGy. The present dosimetry system having advantages of high sensitivity with immediate readout of dose values, low cost, and easy construction would widely be used as an alternative to TLD dosimeters for organ and skin dose measurements in CT and other diagnostic radiology. [DOI: 10.1118/1.1489042]

Key words: medical exposure, organ dose, x-ray CT, diagnostic radiology, pin silicon photodiode radiation sensor

I. INTRODUCTION

Patient exposure from diagnostic x rays must be denoted by tissue or organ dose and the effective dose, where the latter—established by the International Commission on Radiological Protection in 1990—is calculated from the dose values for critical organs. One common method of estimating organ doses is through Monte Carlo simulations of photon interactions within a simplified mathematical model of the human body.[1,2] Calculated dose values, however, should be verified by examinations using anthropomorphic or cylindrical phantoms and the same exposure conditions as the calculation.[3]

Measurements of tissue or organ doses due to medical exposure have been performed by exclusively using thermoluminescent dosimeters (TLDs) inserted in anthropomorphic phantoms[4–7] consisting of tissue equivalent materials. Although TLDs have the advantages of small size for phantom use, angular independence of response, tissue equivalence, and nearly flat energy response for the types of BeO and LiF,[8] they have disadvantages of indirect reading, poor reliability of dose values because of large scattering of measured values among their samples, and a low sensitivity for the types of BeO and LiF. In recent years a metal–oxide–semiconductor field effect transistor (MOSFET) dosimeter was devised as an alternative to TLDs for the measurement of entrance surface dose in diagnostic radiology.[9] The sensitivity of the MOSFET dosimeter, however, was not high enough with a measurable dose of more than 1.5 mGy. Hence the dosimeter would not be utilized for the measurement of organ doses.

Pin silicon photodiodes have been used with x- and γ-ray spectroscopy with a high energy resolution.[10–12] We tried to apply the photodiodes to a highly sensitive and small sized x-ray sensor used in a diagnostic energy region. In the present paper we describe the development of a dosimetry system using commercially available pin silicon photodiodes as the sensor for measuring organ doses delivered by x-ray CT and other diagnostic radiology.

II. DESCRIPTION OF THE DOSIMETRY SYSTEM

A. Pin silicon photodiode sensor

Pin silicon photodiodes used as the x-ray sensor of the dosimetry system are those of Hamamatsu S2506-04, details of which are shown in Fig. 1(a). The photodiode with a relatively large sensitive area of 2.8×2.8 mm^2 has a low cost—about 2 US dollars in Japan—and is molded out of black resin, 2.7 mm thick, for infrared spectral response. It was found that x-ray detection efficiency for a single photodiode of this type largely differed by the incident direction of x rays—several times greater on the plane of incidence than on the back side—because of metal backing behind a silicon wafer. To obtain the same detection efficiency without depending on the incident direction of x rays, two photodiodes were glued together back to back with epoxy cement, and they were used as a single sensor with parallel connection. The photodiodes were wrapped up in 15-μm-thick aluminum

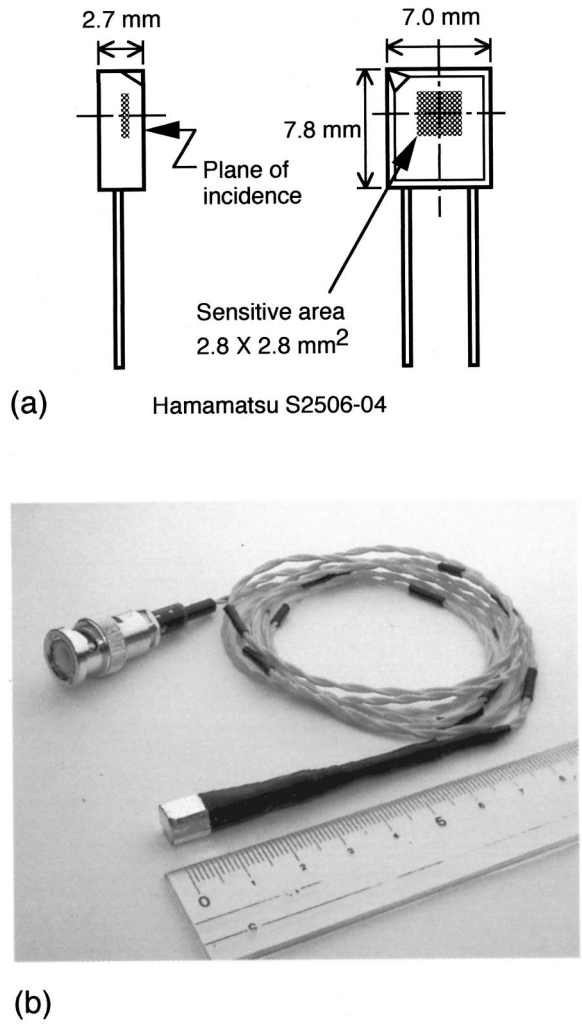

FIG. 1. Pin silicon photodiode used (a), and a photodiode x-ray sensor with a pair of twisted carbon-fiber cables (b). The fine scale on the rule is in millimeters.

foil for electromagnetic shielding and connected to a pair of twisted carbon-fiber cables, 1 mm in diameter and about 150 $\Omega\,m^{-1}$ in resistance. The tail of the photodiodes, the junction of the photodiodes and the cables, was covered with a thermal-contraction black plastic tube for mechanical reinforcement, as seen in Fig. 1(b). The carbon fiber cables were used because of the tissue equivalence of cable material, which fact is significant when many photodiode sensors with cables are placed in an anthropomorphic phantom. Since the cables with resistance were likely to pick up external noise the length of the cables was made as short as possible by using a preamplifier placed at the phantom side.

B. Electronics

A 16-channel dosimetry system consisting of 16 identical photodiode sensors and electronic circuits was devised. The signal current generated by x-ray incidence on a photodiode sensor was fed through a 1.5 m carbon-fiber cable to a preamplifier consisting of an operational-amplifier current-to-voltage converter and a voltage-follower. A relatively large rise time constant of 0.1 s of the output voltage was determined to suppress ac line noise of 60 Hz to a negligible level.

Each output voltage from the 16-channel preamplifier was fed through a 20 core cable of 5 m long to a current integrator placed in the control room, and integrated to the total charge proportional to the dose absorbed by each photodiode sensor. The sensitivity or the measurable dose range of the system could be changed by five times selecting the time constant of the current integrator, i.e., a 0.02–20 mGy range for a higher sensitivity, and a 0.1–100 mGy range for a lower sensitivity. In the following experiments the higher electronic sensitivity was always selected.

Analog output voltage of each current integrator was converted to a digital value with an analog-to-digital converter (ADC) with 16 input and output channels and a quantum error of 2.5 mV. Data were acquired on a personal computer with a sampling time of 0.1 s, and voltage increases from the beginning of x-ray irradiation were traced. The maximum or plateau voltages were used to calculate dose values by using calibration factors experimentally determined for each channel.

III. CHARACTERISTICS OF THE DOSIMETERY SYSTEM

Output linearity, and dose rate, x-ray energy, and angular dependence of the sensitivity were assessed for the present dosimetry system by making exposures of one of 16 photodiode sensors. The same electronic channel was always used in the experiments to remove the influence of gain or sensitivity discrepancy between the channels. Experiments were carried out by using an x-ray generator for medical radiography with an x-ray tube with 2.2 mm Al inherent filtration and a sequential CT scanner, Toshiba TCT 300, with an x-ray tube with a bow-tie filter of 8 mm Al total filtration at the x-ray beam center.

Output linearity, dose rate, and energy dependence of system sensitivity were measured in free air by setting the sensors on a thin plate of polystyrene foam to be oriented to have the plane of incidence of the photodiodes facing the x-ray tube of the x-ray generator for medical radiography. Dose calibrations were made against a Radcal 1015 dosimeter with a 6 cm^3 ion chamber attached, which was placed adjacent to a photodiode sensor, a few centimeters apart, at the same distance from the x-ray tube in an irradiation field. The ion chamber dosimeter is a tertiary standard, calibrated at a laboratory of the Japan Quality Assurance Organization in April 2001, where dosimeter readings were calibrated to exposure dose values at nine points of effective or equivalent photon energies[13] from 20 to 72 keV. The values of exposure dose in the unit of roentgen obtained with the ion chamber dosimeter were converted to the values of absorbed dose for soft tissue by using the ratio of mass energy absorption coefficient of soft tissue (ICRU-44)[14] to that of air at the effective energy of x rays used. This is because absorbed doses for almost all organs excepting bones would be approximated to those for soft tissue.

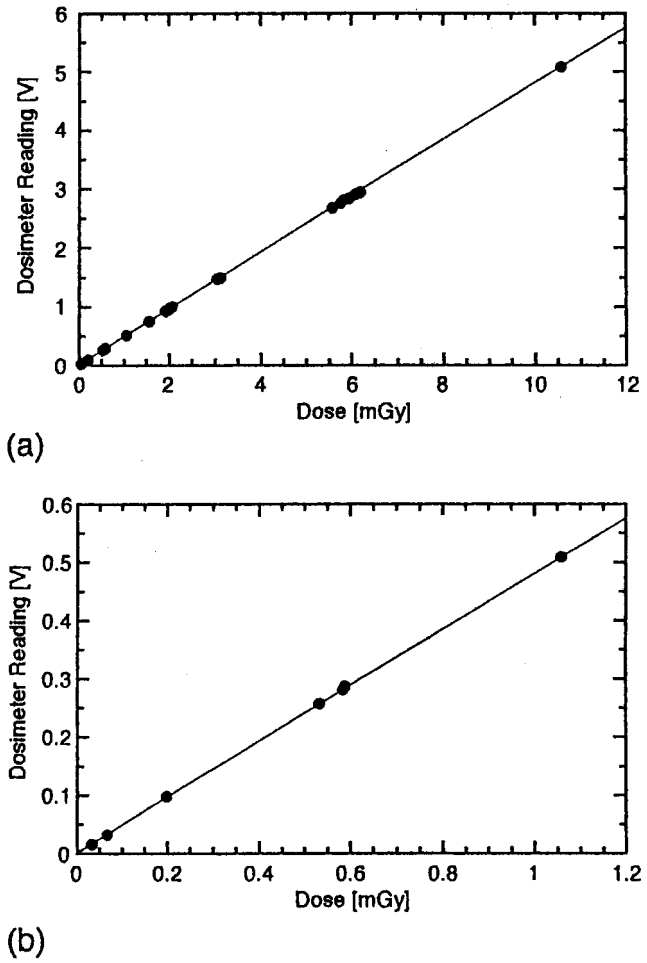

FIG. 2. Output linearity of the dosimetry system. (b) is the same as (a), but ten times magnified at the origin.

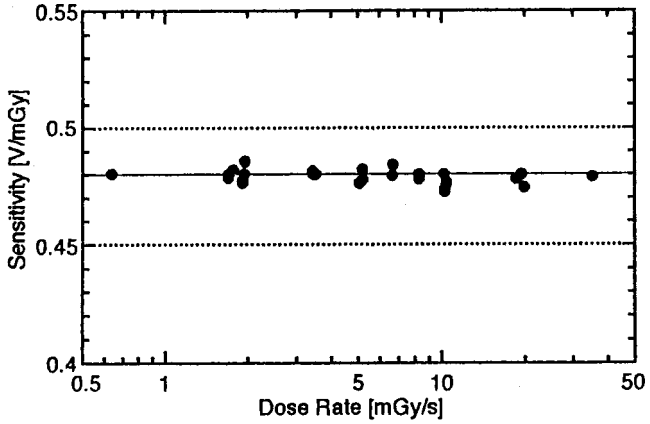

FIG. 3. Dose rate dependence of system sensitivity.

Output linearity and dose rate dependence of system sensitivity were measured using the x-ray generator at a tube voltage of 120 kV—an effective energy of 36 keV—and an intensity range between 1 and 60 mA s with focus-to-sensor distances (FSDs) of 90, 120, and 200 cm. The effective energy was determined from the half-value layer of aluminum measured with the Radcal 1015 ion-chamber dosimeter. Results are shown in Figs. 2 and 3, respectively, for output linearity and for dose rate dependence of system sensitivity. It is seen from Figs. 2(a) and 2(b) that output linearity was excellent over a dose range from 0.03 to more than 10 mGy, three orders of magnitude. Although no bias voltage was applied to photodiode sensors uniform sensitivity was obtained, as seen in Fig. 3, within 2% error up to a high dose rate of 35 mGy s^{-1} that would be expected in CT examinations.

The minimum detectable organ dose could be estimated using a sensitivity of approximately 0.48 V/mGy as seen in Fig. 3 and a quantum error of the ADC used of 2.5 mV to be 0.02 mGy with 25% uncertainty.

The energy spectra or effective energies of x rays observed in a phantom would differ from those in free air because of absorption and scattering of x rays in the phantom. Hence the use of the calibration factor—the inverse of the sensitivity—at the effective energy measured in free air would produce errors in dose values if the system has no flat energy response.

X-ray energy dependence of the sensitivity was measured across a range of tube voltage of 40–120 kV in 10 kV intervals and at 125 kV, where x-ray irradiation was carried out with a FSD of 100 cm and an x-ray intensity of 60 mA s. Results are shown in Fig. 4(a), where the sensitivities were plotted as a function of the effective energy measured at each tube voltage for generalization. The range of the effective energy was between 23.5 keV at 40 kV tube voltage and 36.5 keV at 125 kV. It was found from Fig. 4(a) that the sensitivity changed 3% at the maximum between 27 and 36.5 keV—between 60 and 125 kV—though it changed more than 7% between 23.5 and 27 keV—between 40 and 60 kV. Energy response of the photodiode sensor was also measured for larger effective energies used in x-ray CT by using Al filters attached to the window of the x-ray tube at a constant tube voltage of 120 kV. Effective energies of x-rays in this case increased from 36 to 72 keV, corresponding to the energy range used in CT scanners, with increasing Al filter thickness to a maximum of 40 mm. X-ray irradiation was carried out with a FSD of 100 cm and an x-ray intensity of 100 mA s. Results are shown in Fig. 4(b). It was found from Fig. 4(b) that the sensitivity decreased at a rate of 9.5% /10 keV by the increase of the effective energy in a range between 50 and 70 keV.

Photodiode sensors placed in a phantom are exposed not only to direct x rays from an x-ray tube but also to scattered x rays coming from all angles. In the case of CT examinations direct x rays come from circumference with a uniform intensity. Hence dosimeters for phantom use must have the flat angular response.

The angular dependence of the sensitivity was measured for a couple of different x-ray effective energies by using the x-ray generator for medical radiography for lower energy and the CT scanner for higher energy. It was measured around the axis of the sensor, the lateral direction, as seen in Fig. 5(a), and on the plane comprising the head and tail and the plane of incidence of the sensor, the longitudinal direc-

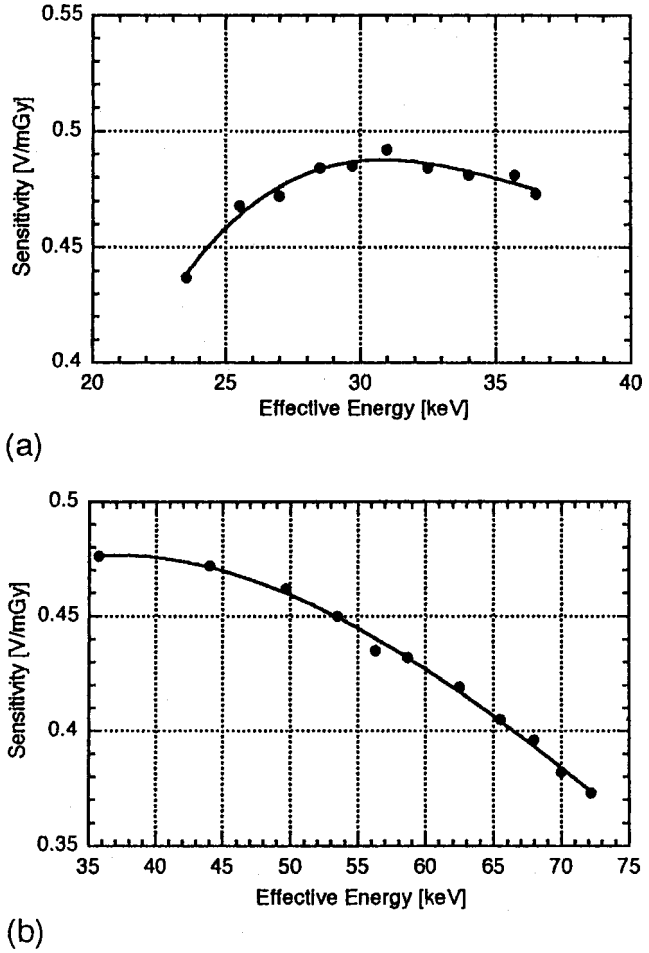

FIG. 4. X-ray energy dependence of system sensitivity for (a) a lower and (b) a higher effective energy region, where the sensitivity was measured with the higher sensitivity range. Sensitivity decreases by a factor of 5 for the lower sensitivity range.

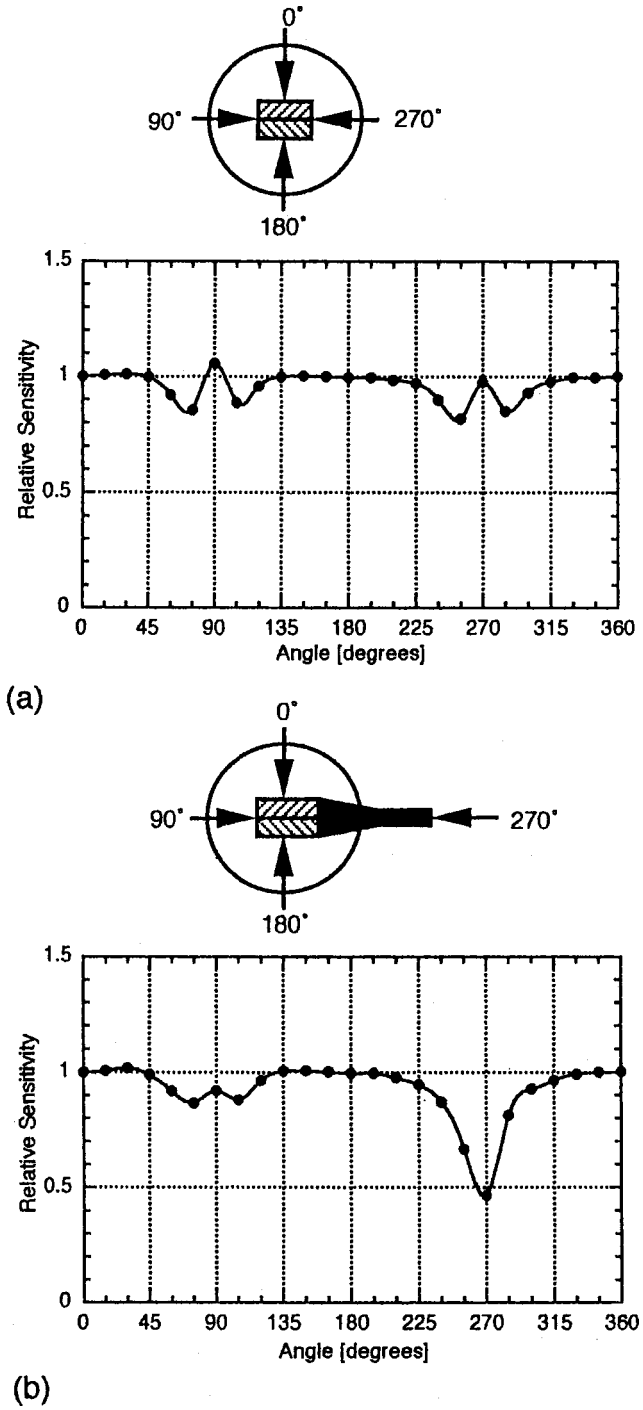

FIG. 5. Angular response of the photodiode sensor for (a) lateral and (b) longitudinal directions measured at a tube voltage of 80 kV, an effective energy of 30 keV. Incident angles of x rays for lateral and longitudinal directions are shown.

tion, as seen in Fig. 5(b). The origin or an angle of 0° was fixed to the orientation of x rays facing one of the planes of incidence of the photodiode sensor.

Angular dependence of the sensitivity observed for lower energy of x rays is shown in Figs. 5(a) and 5(b) for lateral and longitudinal directions, respectively. These were measured by the exposure of the sensor in free air at 15° intervals using the x-ray generator at a tube voltage of 80 kV—an effective energy of 30 keV—and an intensity of 30 mAs with a FSD of 100 cm. In Figs. 5(a) and 5(b) the sensitivity was normalized at 0°. It is seen from Fig. 5(a) that relative sensitivity was approximately flat though it was slightly waved around 90° and 270° with a maximum deviation of 18%. Approximately flat angular response is also seen in Fig. 5(b) except between 240° and 290° where the relative sensitivity dropped to 46% at 270° or the tail of the sensor.

Angular response for higher energy of x rays was measured using the sequential CT scanner at a tube voltage of 120 kV—an effective energy of 52.5 keV—and a tube current of 55 mA. A photodiode sensor was supported with a thin bar of polystyrene foam in free air at the center of rotation and in an x-ray beam of 10 mm width. Preamplifier output voltage corresponding to the sensitivity was measured as a function of time in a single scan of 4.5 s with a digital oscilloscope. The uniformity of x-ray intensity in a single scan was confirmed with a plastic scintillation detector with cylindrical symmetry[15] placed in place of the photodiode sensor. Figures 6(a) and 6(b) show observed oscillograms corresponding to the angular dependence of the sensitivity for lateral and longitudinal directions, respectively. In Figs.

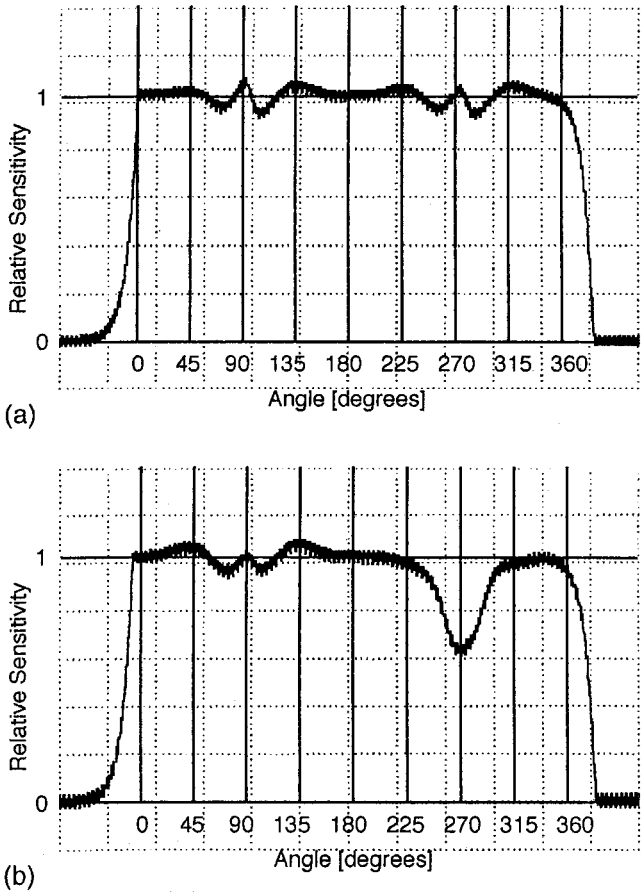

FIG. 6. Oscillograms of the preamplifier output voltage corresponding to the sensitivity as a function of time in a single scan of 4.5 s measured with a sequential CT scanner, Toshiba TCT 300, at a tube voltage of 120 kV, an effective energy of 52.5 keV. These oscillograms correspond to the angular response of the photodiode sensor for (a) lateral and (b) longitudinal directions, respectively, where abscissas are converted from time in a scan to the incident angles of x rays.

6(a) and 6(b) abscissas are converted from time in a scan to the incident angle of x rays, where signals at $<0°$ and $>360°$ are due to the overrun of x-ray tube revolution of approximately 30° and a relatively slow rise time—time constant of 0.1 s—of the preamplifier output voltage, respectively. It is seen from Fig. 6(a) that relative sensitivity was approximately flat though it was slightly waved around 90° and 270° with a maximum deviation of 8.5%. The average sensitivity was coincided to the sensitivities at 0° and 180°. Approximately flat angular response is also seen in Fig. 6(b) except between 245° and 295° where the relative sensitivity dropped to 61% at 270°.

IV. APPLICATION TO CT DOSE MEASUREMENTS

Applicability of our dosimetry system to the measurement of a wide range of dose values was examined by the measurement of dose profile along the axis of a thoracic phantom undergoing CT chest examination. The phantom made of water equivalent MixDP[16] and a small density of cork for the lung was designed to have an average lung size of a Japanese adult male and a uniform cross section along the axis of the

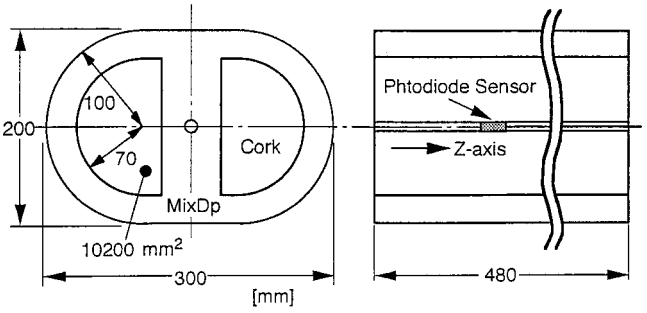

FIG. 7. Thoracic phantom designed to have an average lung size of a Japanese adult male. A photodiode sensor was installed at the center of the phantom with the axis of the sensor parallel to the z axis.

phantom, over a length of 480 mm, where the MixDP is a kind of solid water with a mass density of 1.000 $g\,cm^{-3}$ and an electron density of $3.382\times10^{23}\,g^{-1}$ close to that of water of $3.343\times10^{23}\,g^{-1}$. The construction of the phantom is shown in Fig. 7. One of the photodiode sensors was installed at the center of the phantom with the axis of the sensor parallel to the z axis, the axis of the phantom, where the phantom was placed on the bed of the sequential CT scanner, Toshiba TCT 300. A dose profile along the z axis was measured over a scan length of 300 mm around the sensor. The CT scanner was used with a tube voltage of 120 kV—an effective energy of 52.5 keV—a tube current of 55 mA, and a 10 mm beam width. Output voltages derived from the current integrator were converted into absorbed doses using the sensitivity obtained from Fig. 4(b) at an effective energy of 52.5 keV. A dose profile obtained is shown in Figs. 8(a) and 8(b), where Fig. 8(a), the dose profile of the central region of the total scan length, is the same as Fig. 8(b), the dose profile of the peripheral region. It is seen from Fig. 8 that dose values ranged over two orders of magnitude from less than 0.2 to 12 mGy, and that they continuously changed in the scan region indicating the reliability of measured dose values with small static errors.

Computed tomography dose index (CTDI) value was also measured with a standard CT ion chamber (Radcal mdh 10X5-10.3CT) with an effective length of 100 mm. The chamber was installed in the phantom at the point of the photodiode sensor in place of the sensor, and the center of the chamber was exposed to one-scan x-ray beam from the same CT scanner with the same operational conditions. The CTDI value obtained was 28.8 mGy with an error of several percent, the value of which would correspond to the dose value obtained by the integration of the dose profile of fig. 8(a) between -50 and 50 mm and divided by 10 mm beam width. The integrated dose value of 26.2 mGy calculated coincided with the CTDI value measured with the CT ion chamber within 10% error.

Comparison of integrated dose values calculated from dose profiles with CTDI values measured with the Radcal CT ion chamber was carried out at different tube voltages of CT scanner or different x-ray effective energies. Dose profile and CTDI measurements were carried out with the same thoracic phantom and geometry as shown in Fig. 7 but with

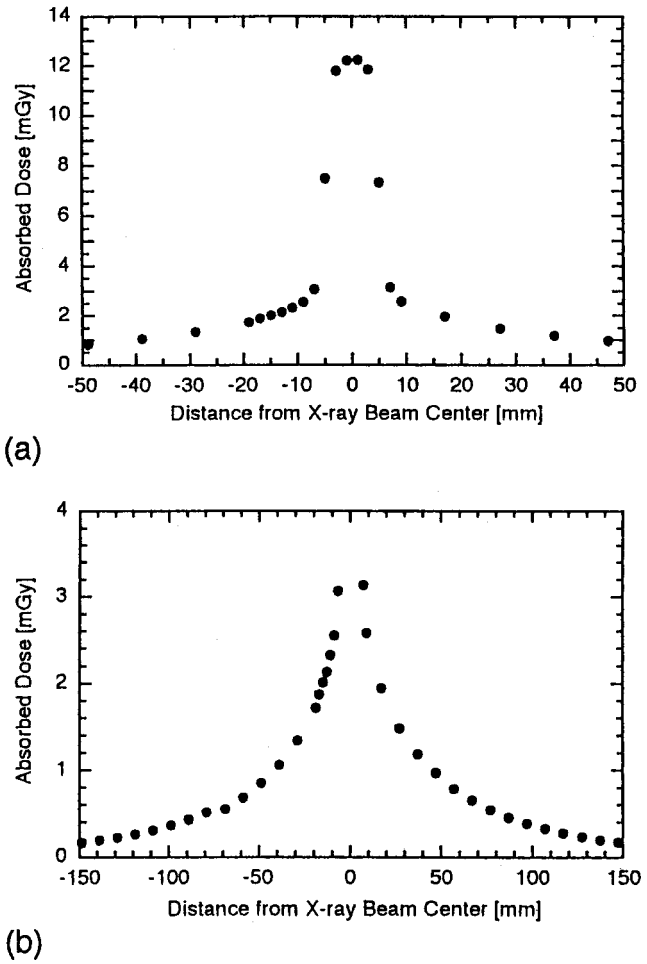

FIG. 8. Dose profiles along the *z* axis of the phantom for (a) the central region and (b) the peripheral region of total scan length of 300 mm. These profiles were measured using a sequential CT scanner, Toshiba TCT 300, with a tube voltage of 120 kV, an effective energy of 52.5 keV, a tube current of 55 mA, and 10 mm beam width.

another CT scanner, Toshiba Asteion. The CT scanner was used with tube voltages of 80, 120, and 135 kV corresponding to effective energies of 39.5, 48, and 51 keV, respectively, and with a tube current of 200 mA at 0.75 s per scan and a 10 mm beam width. Table I shows integrated dose values obtained by the integration of dose profiles between −50 and 50 mm and divided by 10 mm beam width and CTDI values measured with the CT ion chamber possessing 100 mm effective length. It is seen in Table I that integrated dose values and CTDI values coincided at each tube voltage within 1%–5% error.

TABLE I. Integrated dose values calculated from dose profiles and CTDI values measured with the Radcal CT ion chamber possessing 100 mm effective length. These were measured at different tube voltages of the Toshiba Asteion CT scanner.

Tube voltage (kV)	Effective energy (keV)	Integrated dose (mGy)	CTDI value (mGy)
80	39.5	6.09	5.82
120	48	18.3	18.1
135	51	23.7	24.6

V. DISCUSSION

In a water phantom the effective energy of x rays in a beam would be increased or decreased[17] by several kiloelectron volts because of the selective absorption of the low energy part of the spectrum and of selective Compton scattering of the high energy part of the spectrum. On the contrary the effective energy of x rays at the point distant from the beam would be decreased[18] since x rays incident on that point are solely those scattered in the phantom. For the lower x-ray energy region used in medical radiography dose error due to energy response of our dosimetry system was estimated to be within 6% from Figs. 4(a) and 4(b), where a range of the effective energy was assumed to be between 25 and 50 keV in a phantom. For the higher x-ray energy region used in x-ray CT dose error due to the energy response in Fig. 4(b) would be within 10%, where the change of the effective energy was assumed to be within 10 keV in an effective energy range between 40 and 70 keV. As described previously CT dose values obtained by the integration of dose profiles and divided by the x-ray beam width coincided with CTDI values measured with an energy independent CT ion chamber within a few to 10% error. This might indicate that the under- or overestimation of dose values due to the energy response of the present dosimeter system would not be greater than several percent for the x-ray energy region used in CT. In the case of entrance surface or skin dose measurements dose error due to the energy dependence of system sensitivity would be negligible.

Relative sensitivities with small angular dependence were obtained as seen in Figs. 5 and 6, except at the tail of the sensor or at 270° for the longitudinal direction across a range of about 50°. If x rays come from all angles uniformly dose values estimated would be underestimated by 7.5% and 3% for the lower and the higher effective energy, respectively, since calibration factors were measured at 0°. It is not, however, direct x rays that enter the head and tail of the photodiode sensors but scattered in the phantom since the sensors are placed in a phantom with the plane of incidence facing the x-ray tube for medical radiography or with the axis of the sensors parallel to the axis of rotation of CT scanners. Since solid angle is no more than 0.047 for a range of 50° and scattered weak x rays solely come at around 270°, influence of the sensitivity drop at the tail of the sensor would be negligible to the estimation of dose. Symmetry dose values observed at the same distances from the x-ray beam, as seen in Fig. 8, indicate the negligible effect of sensitivity drop at 270° to the total dose values.

The present sensors are somewhat larger in size and they have carbon fiber cables behind them. To position the sensors inside a particular organ site of an anthropomorphic phantom the section of the phantom comprising the organ must be drilled with 10 mm diameter parallel to the axis of the phantom. Carbon fiber cables should be led to the back of the phantom through a groove made at the surface of the same

phantom section. Drilled holes and grooves for the cables must be filled with tissue or water equivalent resin as MixDP after sensors were positioned in the section of the phantom. An anthropomorphic phantom with 16 photodiode x-ray sensors installed in critical organ sites would be used to estimate tissue or organ doses and the effective doses to patient exposure from diagnostic x rays.

VI. CONCLUSIONS

The dosimetry system using pin silicon photodiodes as the sensor is an alternative to the use of TLD dosimeters in the measurement of organ doses in CT and other diagnostic radiology. The system had linear dose and flat dose rate responses, a minimum detectable dose of 0.02 mGy with 25% error and approximately flat angular response though it had relatively large x-ray energy dependence of the sensitivity. Dose error due to the energy dependence was evaluated to be within several percent for the x-ray energy region used in medical radiography and x-ray CT if dose values evaluated at the effective energy of x rays in the air were used for the values of dose in the phantom.

The immediate readout of the organ doses is the major advantage of the system. Although the sensors are not small enough for phantom use, high sensitivity and reliability of the system allows us to use the system successfully for the measurements of organ and skin doses in CT and other diagnostic radiography.

[a]Electronic mail: aoyama@met.nagoya-u.ac.jp

[1] M. Zankl, "Methods for assessing organ doses using computational models," Radiat. Prot. Dosim. **80**, 207–212 (1998).
[2] C. H. McCollough and B. A. Schueler, "Calculation of effective dose," Med. Phys. **27**, 828–837 (2000).
[3] M. Caon, G. Bibbo, and J. Pattison, "A comparison of radiation dose measured in CT dosimetry phantoms with calculations using EGS4 and voxel-based computational models," Phys. Med. Biol. **42**, 219–229 (1997).
[4] R. L. Mini, P. Vock, R. Mury, and P. P. Schneeberger, "Radiation exposure of patients who undergo CT of the trunk," Radiology **195**, 557–562 (1995).
[5] K. Nishizawa, T. Maruyama, M. Takayama, K. Iwai, and Y. Furuya, "Estimation of effective dose from CT examination," Nippon Acta Radiologica **55**, 763–768 (1995).
[6] T. Maruyama, K. Iwai, K. Nishizawa, Y. Noda, and Y. Kumamoto, "Organ or tissue doses, effective dose and collective effective dose from x-ray diagnosis, in Japan," Radioisotopes **45**, 761–773 (1996).
[7] G. Giacco, V. Cannata, C. Furetta, F. Santopietro, and G. Fariello, "On the use of pediatric phantoms in the dose evaluation during computed tomography (CT) thorax examinations," Med. Phys. **28**, 199–204 (2001).
[8] G. Shani, *Radiation Dosimetry Instrumentation and Methods* (CRC Press, Ann Arbor, 1991), pp. 63–116.
[9] D. J. Peet and M. D. Pryor, "Evaluation of a MOSFET radiation sensor for the measurement of entrance surface dose in diagnostic radiology," Br. J. Radiol. **72**, 562–568 (1999).
[10] N. Markevich, I. Gertner, and J. Felsteiner, "Low energy x-ray and γ spectroscopy using silicon pin photodiodes," Nucl. Instrum. Methods Phys. Res. A **269**, 219–221 (1988).
[11] K. Aoki and M. Koyama, "A silicon diode in a thimble-type mount for measurement of diagnostic x-ray spectra," Phys. Med. Biol. **35**, 1505–1517 (1990).
[12] M. C. Silva, S. B. Herdade, P. Lammoglia, P. R. Costa, and R. A. Terini, "Determination of the voltage applied to x-ray tubes from the bremsstrahlung spectrum obtained with a silicon PIN photodiode," Med. Phys. **27**, 2617–2623 (2000).
[13] F. H. Attix, *Introduction to Radiological Physics and Radiation Dosimetry* (Wiley, New York, 1986), p. 226.
[14] J. H. Hubbell and S. M. Seltzer, *Tables of X-Ray Mass Attenuation Coefficients and Mass Energy-Absorption Coefficients 1 keV to 20 MeV for Elements $Z=1$ to 92 and 48 Additional Substances of Dosimetric Interest*, NISTIR 5632 (National Institute of Standards and Technology, Gaithersburg, MD, 1995).
[15] T. Aoyama, S. Koyama, and H. Maekoshi, "Precise measurement of CT exposure dose with a scintillation-point dosimeter," Jpn. J. Radiol. Technol. **56**, 87–94 (2000).
[16] Y. Onai and G. Kusumoto, "Trial production of a water-equivalent solid phantom material," Nippon Acta Radiologica **19**, 1012–1016 (1959).
[17] K. W. Senstrom and J. F. Marvin, "Ionization measurements with bone chambers and their application to radiation therapy," Am. J. Roentgenol. Radium Ther. **56**, 759–770 (1946).
[18] G. Hettinger and K. Lidén, "Scattered radiation in a water phantom irradiated by roentgen photons between 50 and 250 keV," Acta Radiol. (1921-1962) **53**, 73–92 (1960).